# Silver and Mercury Probing of Deoxyribonucleic Acid Structures in the Filamentous Viruses fd, If1, IKe, Xf, Pf1, and Pf3†

Arturo Casadevall* and Loren A. Day

ABSTRACT: $Ag^+$ binding and $Hg^{2+}$ binding to both double-stranded DNA (dsDNA) and single-stranded DNA (ssDNA) have been examined in some detail, and the results have been applied to study the structures of circular ssDNA in several filamentous viruses. It has been known for some time that $Ag^+$ and $Hg^{2+}$ bind to the bases of DNA producing characteristic large changes in absorbance and circular dichroism (CD) spectra, as well as changes in sedimentation rates. In the case of $Ag^+$, it is known that there are three modes of binding to isolated dsDNA, referred to as types I, II, and III. Type III binding, by definition, occurs when $Ag^+$ binds to Ag–dsDNA complexes having sites for binding types I and II extensively occupied, if not saturated. It produces CD spectra, assigned in this study, and absorbance spectra that are isosbestic with those of the Ag–dsDNA complexes present prior to its onset. In phosphate buffers binding is restricted to types I and II, whereas in borate buffers weaker type III binding can occur. Characteristics of types I, II, and III were observed for the DNAs in fd, If1, IKe, and Xf, but not for those in Pf1 and Pf3. Similarly, many of the spectral changes seen when $Hg^{2+}$ binds to isolated double-stranded DNA are mimicked by $Hg^{2+}$ binding to the DNAs within fd, IKe, If1, and Xf, but not for those in Pf1 and Pf3. The $Ag^+$ and $Hg^{2+}$ results indicate the presence of right-handed DNA helices in fd, If1, IKe, and Xf, with the two antiparallel strands of the covalently closed single-stranded DNAs having the bases directed toward the virion axes. For Pf1 and Pf3, $Ag^+$ and $Hg^{2+}$ binding cause large absorbance changes but only small CD changes. The very different results for Pf1 and Pf3 are consistent with the presence of inverted DNA structures (I-DNA) with the bases directed away from the structure axes, but the two structures differ from one another. Sedimentation velocity changes with $Ag^+$ and $Hg^{2+}$ binding strongly suggest structural linkages between the DNA and the surrounding protein sheath in each of the viruses.

The virions of fd, Xf, If1, IKe, Pf1, and Pf3 are long and slender filaments in each of which a covalently closed loop of single-stranded DNA is folded back upon itself and held by thousands of major coat protein subunits. The virions range from 0.7 to 2.0 μm in length. A few molecules each of different minor coat protein subunits are at the ends. Because of the single strandedness and fold back of the DNA, there are two antiparallel chains which are not necessarily base paired. The structure problem is to understand how the DNA and protein components are packed together in such viruses, and it involves considerations of how the two DNA strands interact with each other and with the protein sheath that surrounds them. It is now clear from several studies that the DNA packing is different from virus to virus (Day & Wiseman, 1978; Day et al., 1979; Casadevall & Day, 1982; Thomas et al., 1983; Cross et al., 1983; Marzec & Day, 1983; Putterman, 1983). In one of these studies $Ag^+$ was used to probe the DNA structures in four of the viruses (Casadevall & Day, 1982). The changes induced by $Ag^+$ in the CD[1] and ultraviolet absorbance spectra of fd and Xf were similar to each other and similar to changes for isolated single- and double-stranded DNAs, both linear and superhelical. However, the changes induced by $Ag^+$ on Pf1 and Pf3 were very different. It was concluded that the DNAs in fd and Xf both have approximately the same pitch, that the bases are directed toward the structure axes, and that both helices are right-handed. Evidence from other sources and other considerations (Day et al., 1979; Cross et al., 1983; Marzec & Day, 1983; Putterman, 1983) indicate that the antiparallel chains of DNA in Pf1 and in Pf3 have inside-out or inverted structures (I-DNA) with phosphates in and bases out.

Both $Ag^+$ and $Hg^{2+}$ bind to the DNA bases, causing large changes in absorbance and circular dichroism spectra [a recent review of metal binding to DNA is that by Marzilli et al. (1980)], and these effects have been used by several workers to probe DNA structures in viruses and nucleosomes (Minchenkova et al., 1969; Dorne & Hirth, 1970; Simpson & Sober, 1970; Ding & Allen, 1980a). For both $Ag^+$ and $Hg^{2+}$ we have observed changes in absorbance and CD spectra and sedimentation properties which provide information about the DNA structures. The results show close structural similarities for the DNAs in four of the six filamentous viruses, but very different structures for the DNAs in the other two. The results also strongly suggest structural linkage between the DNA helices and surrounding protein sheath in these viruses. In addition, the results help define conditions for preparing metal complexes of the viruses for study by other structural techniques such as electron microscopy, X-ray diffraction, and Raman spectroscopy.

## Materials and Methods

PM2 DNA, a covalently closed circular double-stranded DNA, was isolated from the PM2 bacteriophage by multiple extractions with phenol. The phage itself was prepared from a lysate of its host BAL31 by precipitation in 4.3% poly(ethylene glycol) and 0.24% sodium dextran sulfate, resuspended in neutral Tris-HCl buffer, and purified by CsCl gradient centrifugation. Linear double-stranded PM2 DNA was generated by restriction cleavage of superhelical PM2

† From The Public Health Research Institute of the City of New York, New York, New York 10016. *Received February 23, 1983.* This work was supported by National Institutes of Health Research Grant AI 09049 (L.A.D.). A.C. is supported by Medical Scientist Training Grant 5-T32-GM07308 in the New York University School of Medicine.

[1] Abbreviations: CD, circular dichroism; Tris, tris(hydroxymethyl)-aminomethane; DTT, dithiothreitol; $Hg(OAc)_2$, mercuric acetate; dsDNA, double-stranded DNA; ssDNA, single-stranded DNA; deg, degree; SDS, sodium dodecyl sulfate.

0006-2960/83/0422-4831$01.50/0 

DNA with endonuclease *Hpa*II which cleaves at only one site. The DNA incubated with *Hpa*II (BRL lot no. 06311) in a 20 mM Tris-HCl, pH 7.4, 7.0 mM $MgCl_2$, and 1.0 mM DTT buffer at 37 °C for 2 h; greater than 99% cleavage was obtained as measured by agarose gel electrophoresis. Single-stranded DNA was prepared by multiple phenol extractions of the filamentous phage fd. The DNA samples were dialyzed against the desired buffers at 4 °C. The buffers used were 0.05 M and 0.10 M phosphate at pH 7.0 and 0.15 M borate at pH 7.5 and pH 8.6. DNA concentrations were determined by absorbance spectra measured in a Cary 219 spectrophotometer by using extinction coefficients of 22.6 $mg^{-1}$ $cm^2$ for fd ssDNA and of 20.0 $mg^{-1}$ $cm^2$ for dsDNA at 259 nm. Difference absorbance spectra were obtained in the same instrument. The viruses were isolated and purified with modifications of the standard poly(ethylene glycol) precipitation and CsCl gradient centrifugation techniques of Yamamoto et al. (1970), as described in part elsewhere (Berkowitz & Day, 1980; Casadevall & Day, 1982). Virus concentrations were determined from their absorbances by using extinction coefficients listed elsewhere for fd, Xf, Pf1, and Pf3 (Casadevall & Day, 1982) and 3.5 $mg^{-1}$ $cm^2$ for IKe and If1.

The Ag–virus and Ag–DNA complexes were prepared as described in our previous paper (Casadevall & Day, 1982). The $Hg^{2+}$ complexes were prepared by adding mercuric acetate (0.010–0.005 M) in microliter quantities to virus solutions. The $Hg(OAc)_2$ solutions were prepared by dilution of a 0.10 M stock solution containing 0.5% acetic acid. Before addition of $Hg^{2+}$, the virus samples were dialyzed vs. the measuring buffers. The buffers were 0.15 M acetate for pH 5–6 and 0.15 M sodium tetraborate for pH 8–9.8. The solutions were allowed to react overnight at room temperature before any measurements were made.

A modified Cary 60 spectropolarimeter was used to measure the CD spectra. Its gain was adjusted to give +7260 deg $cm^2$ $dmol^{-1}$ at 290 nm for *d*-camphorsulfonic acid (Cassim & Yang, 1969).

Sedimentation rates of the Ag–virus and Hg–virus complexes at various values of *m* were obtained in a Beckman Model E analytical ultracentrifuge equipped with a photoelectric detection system and a multiplexer. In a typical run, three double sector cells having the same concentrations of virus in one sector and buffer in the other were used. One cell contained a virus solution without $Ag^+$ or $Hg^{2+}$ and served to standarize the run, whereas the other two cells contained different concentrations of the metal ions. Least-squares plots of the logarithms of the radical boundary positions vs. time gave relative sedimentation coefficients with average uncertainties of less than 1.5%.

The reversibility of $Ag^+$ and $Hg^{2+}$ binding to DNA and to viruses was determined by removing the metal ions and comparng the materials before and after the titrations. The $Ag^+$ was removed from Ag–virus complexes by dialyzing vs. 0.25–0.50 M NaCl and from Ag–DNA complexes by dialyzing vs. NaCl solutions which were made pH 5–6 by the addition of acetic acid. The $Hg^{2+}$ was removed from Hg–virus complexes by dialysis vs. 0.010 M mercaptoethanol in 0.15 M borate buffer. After the $Ag^+$ and $Hg^{2+}$ ions were removed, the samples were dialyzed against the measuring buffer again. For DNA, the comparisons for reversibility were absorbance and CD spectra as well as migration rates on a 1% gel. For the viruses, the criteria for reversibility were no loss of infectivity and the restoration of original spectra and sedimentation properties. Infectivity assays were done by plating on their respective hosts successive serial dilutions of the titrated virus samples in chloride-containing media.

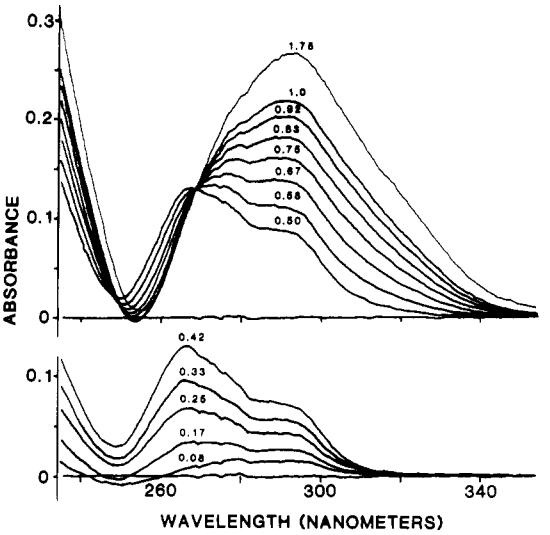


FIGURE 1: Difference absorbance spectra of Ag–dsDNA complexes in 0.15 M borate, pH 8.6, for various values of *m*. The optical path was 1 cm for both the reference and the titration cells. The initial and final DNA concentrations were 0.0234 and 0.0222 mg/mL, with equal volumes of buffer and $Ag^+$ titrant solutions added to reference and titration cells at each step of the titration.

The parameter "*m*" is the ratio of $Ag^+$ or $Hg^{2+}$ added per mole of nucleotide. We have used it as a basis for comparisons of the titrations.

## Results

*$Ag^+$ Binding to Double-Stranded DNA.* Difference absorbance and CD spectra of Ag complexes with superhelical and linear double-stranded DNAs (dsDNA) were found to be very similar if not identical, and in the following no distinction will be made between the spectra for these types of dsDNA. The use of both types of duplex DNA is, however, essential to the conclusions. Although the reaction of $Ag^+$ with DNA is known to be reversible (Yamane & Davidson, 1962), we tested whether $Ag^+$ binding to superhelical DNA caused any nicking that might relax the structure. Agarose gel electrophoresis showed that the PM2 DNA remained superhelical after it had been titrated with $Ag^+$ and the metal ion had been removed.

Figure 1 shows difference absorbance spectra for $Ag^+$ complexes with dsDNA at pH 8.6 in 0.15 M borate buffer from 240 to 350 nm at various values of *m*, the added ratio. Where direct comparisons can be made between our results and those of Jensen & Davidson (1966), the amplitude change for a given value of *m* was within 5% of the change for the same value of *r*, the bound ratio, up to $m = 0.83$. The difference absorbance titration in borate buffer, pH 8.6, shows details observed earlier in unbuffered 0.1 M $NaClO_4$ near pH 8, namely, the isosbestic point at 269 nm and large changes at values of *m* beyond 0.5. In phosphate buffer at pH 7.0 (data not shown), the titration behaves exactly like titrations in borate buffer up to $m = 0.5$ (Figure 1), but then *no further changes at all* are observed for $0.5 < m < 1.0$. Later, at $m \sim 1.2$, pure light scattering contributions appear to begin [our data for PM2 DNA not shown; see Jensen & Davidson (1966)]. In both buffers for $m \leq 0.1$ the absorbance at 250 nm decreases. The effect is slightly more pronounced at pH 7.0 in phosphate buffers [see also Daune et al. (1966)].

The buffer-dependent absorbance effects are paralleled by buffer-dependent CD changes. Figure 2 shows the CD spectra for $Ag^+$ titrations of dsDNA in borate buffer under the conditions of titrations shown in Figure 1. The complexes for *m*

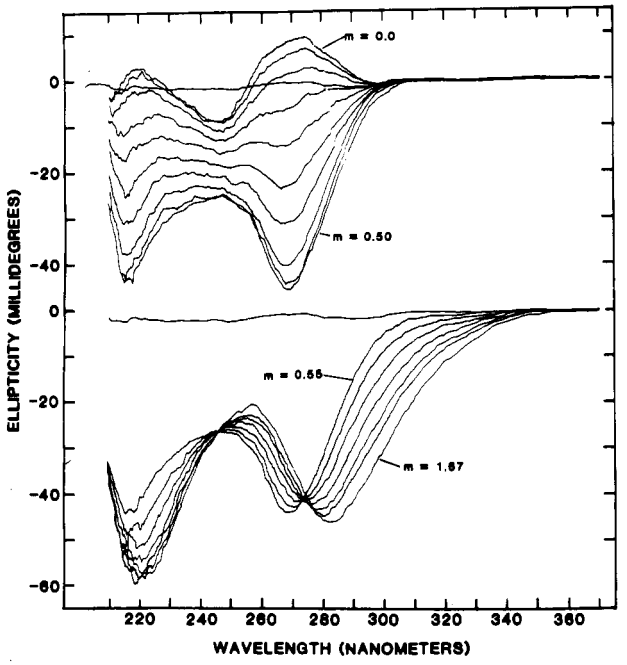


FIGURE 2: CD spectra of superhelical PM2 Ag–dsDNA complexes in 0.15 M borate, pH 8.6, buffer. The unlabeled spectra between $m = 0.0$ and $m = 0.5$ correspond to $m = 0.056$, 0.11, 0.167, 0.22, 0.28, 0.33, 0.39, and 0.44; the spectra between $m = 0.55$ and $m = 1.67$ correspond to 0.67, 0.78, 0.89, 1.0, and 1.1. The initial and final DNA concentrations were 0.0225 ($m = 0.0$) and 0.0215 mg/mL ($m = 1.67$). The path length was 1 cm. The maximum molar ellipticity change at 283 nm induced at $m = 1.67$ was −78 500 deg cm$^2$ dmol$^{-1}$.

< 0.5 develop two enormous negative bands centered at 269 and 216 nm. The spectra for $m < 0.5$ are very similar to those reported by Minchenkova et al. (1969) and by Ding & Allen (1980a,b). However, for $m > 0.5$ the curves change, the negative maximum at 269 nm recedes and a negative maximum near 280 nm develops, isosbestic points occur at 247 and 274 nm, and the band at 216 nm shifts to 220 nm and increases in amplitude. At $m = 1.0$, the CD minima occur at 220 nm and at 280 nm. The CD spectra for $m < 0.5$ have zero amplitudes for wavelengths greater than 300 nm, whereas those for $m > 0.5$ have significant wavelength tails. Previous papers on Ag–DNA complexes at neutral and acidic pHs (Minchenkova et al., 1969; Ding & Allen, 1980a,b) have reported the changes for $m < 0.5$ but not the changes observed in this study for $m > 0.5$. In phosphate buffer at pH 7.0, the CD features seen in Figure 2 for $m < 0.5$ were observed, but the shifts and long wavelength tails for $m > 0.5$ *did not occur.*

*$Ag^+$ Binding to Single-Stranded DNA.* Figure 3 shows a difference absorbance spectra for Ag–ssDNA complexes in a pH 8.6 borate buffer at several values of $m$. They differ somewhat from those of Ag–dsDNA complexes, although the amplitude increases at 280 and 290 nm for $m > 0.5$ are nearly the same for both ssDNA and dsDNA. CD spectra of Ag–ssDNA complexes are shown in Figure 4. For $m < 0.5$, CD spectra are very similar to those of Ag–dsDNA, with negative bands at 220 and 272 nm, but the change in amplitude with $m$ is more linear. For $0.5 < m < 1.0$ the CD spectra of Ag–ssDNA are different from those of Ag–dsDNA, but at $m = 1.0$ they are again different. The Ag–ssDNA spectra show no clear isosbestic point at 274 nm as the minima are shifted to 220 and 283 nm, respectively, in contrast to those for Ag–dsDNA. Also, the ellipticities at the band minima for Ag–ssDNA are about 20% smaller. In a neutral phosphate buffer the results for ssDNA are like those for dsDNA; namely, no band develops at 283 nm with long wavelength tails for $m > 0.5$.

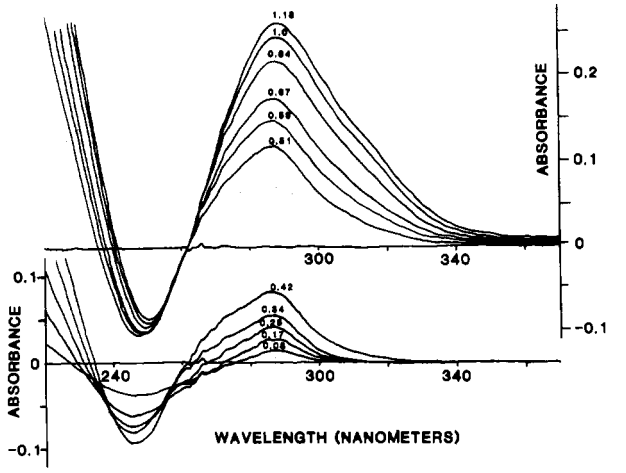


FIGURE 3: Difference absorbance spectra of Ag–ssDNA complexes in a 0.15 M, pH 8.6, borate buffer at various values of $m$ for initial and final DNA concentrations of 0.247 and 0.226 mg/mL, respectively. The optical path was 1 mm. These absorbance curves correspond to the CD curves in Figure 4.

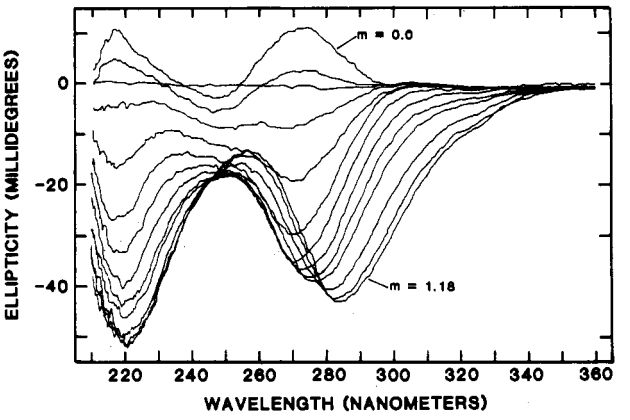


FIGURE 4: CD spectra of Ag–ssDNA complexes in a 0.15 M, pH 8.6, borate buffer. The CD spectra for $m$ values between $m = 0.0$ and $m = 1.18$ have been so labeled; the spectra between them correspond to $m = 0.08$, 0.17, 0.25, 0.34, 0.42, 0.51, 0.59, 0.67, 0.84, and 1.0. The initial and final DNA concentrations were 0.247 ($m = 0$) and 0.226 mg/mL ($m = 1.18$). The optical path was 1 mm. These curves correspond to those of Figure 3. The maximum molar ellipticity change induced by $Ag^+$ at 283 nm was −72 000 deg cm$^2$ dmol$^{-1}$.

*Ag Binding to the fd, Xf, and Pf1 Viruses.* Figure 5 shows the CD spectra of the Ag–fd and Ag–Xf complexes in the borate and phosphate buffers. In phosphate, the minimum occurs at 275 nm and does not shift with increasing $m$. Also, the spectra for $1.0 < m < 3.0$ in phosphate show little of the long wavelength phenomena. However, the CD spectra for $1.0 < m < 3.0$ in borate show long wavelength tails and a shift in the wavelength at which the minimum occurs from 278 to 282 nm. The DNAs in the virions of both Xf and fd thus behave like isolated dsDNA and ssDNA with regard to these buffer-dependent effects. (The spectra for $m < 1.0$ in borate are virtually identical with those we reported in 1982).

The CD spectra of the Ag–Pf1 complexes (Figure 6) also exhibit buffer-dependent changes, but the changes are very different from those observed for dsDNA, for ssDNA, and for the other viruses. In borate, the CD spectra for $1.0 < m < 3.0$ show small positive changes in the 290–350-nm region with long wavelength tails and small negative changes in the 260–290-nm region. In the phosphate buffer, only a small increase in ellipticity is seen at 295 nm.

*Sedimentation Velocity of $Ag^+$ Complexes with the fd, Xf, and Pf1 Viruses.* The addition of $Ag^+$ to the viruses in borate and phosphate buffers led to increases in sedimentation ve-

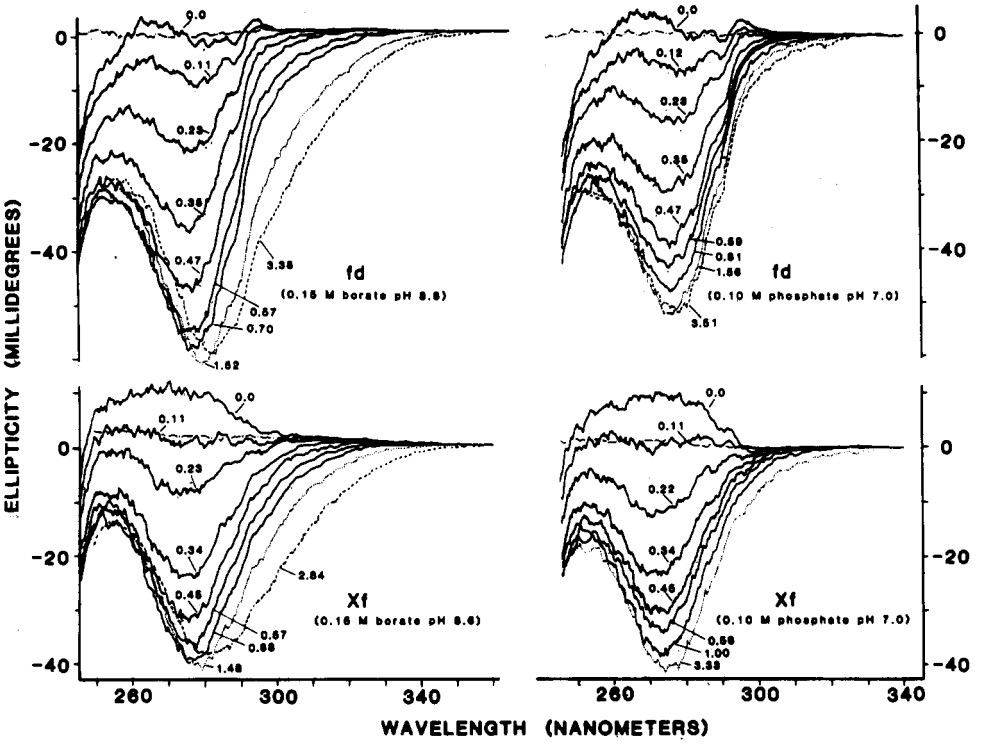


FIGURE 5: CD spectra of Ag–fd and Ag–Xf complexes in a pH 8.6, 0.15 M borate and pH 7.0, 0.10 M phosphate buffers at various values of $m$. The concentrations of fd and Xf were 0.20 and 0.19 mg/mL, respectively, giving DNA concentrations were 0.024 and 0.0245 mg/mL, respectively. Over the course of this study we have observed sample to sample variation in the CD amplitudes of the viruses and their $Ag^+$ complexes. The average total molar ellipticity change (in units of deg cm$^2$ dmol$^{-1}$) at 277 nm between $m = 0$ and $m \sim 1$ was $-72\,000 \pm 5000$ (SD) for fd and $-62\,000 \pm 4000$ (SD) for Xf. Six different fd samples and three different Xf samples were used. Shapes of the spectra have shown little variation. In this figure are the titrations with the largest molar amplitude changes at 277 nm: $-79\,500$ for fd and $-65\,000$ for Xf in borate; in phosphate, $-76\,000$ for fd and $-64\,000$ for Xf. [In Figure 1 of Casadevall & Day (1982), the wavelength markings were inadvertently labeled 5 nm too high, i.e., 330 nm on the abscissa should have read 325 nm etc.]

locity, with the Ag–Xf and Ag–Pf1 complexes exhibiting the largest and smallest increases, respectively (Figure 7). In the phosphate buffer, the sedimentation increases for $m < 1.0$ were almost identical with those in the borate buffer, but only in borate did significant increases in sedimentation velocity occur for $m > 1.0$. The absence of further CD changes in the phosphate buffer is thus paralleled by the absence of sedimentation increases for $m > 1.0$. For all values of $m$ studied, the sedimentation boundaries of the Ag–fd and Ag–Xf complexes were very sharp and no different from those of fd and Xf viruses in the absence of $Ag^+$. The boundary shapes for the Pf1 virus and its $Ag^+$ complexes were also the same, but because of the extreme length of Pf1 (2 $\mu$m), there were significant concentration effects on the sedimentation velocity.

*Reversibility of $Ag^+$ Binding to fd, Xf, and Pf1.* Our previous work showed that $Ag^+$ binding in solutions up to approximately $m = 1.0$ is reversible; original spectra are restored, and infectivity is retained upon removal of the $Ag^+$. Extension of the titrations to $m \sim 3$, however, results in some permanent changes in the virions. For fd, removal of $Ag^+$ from a solution at $m = 3.5$ restored the original spectra, but some material still sedimented too fast, and the plating efficiency was reduced from 20% to 1%. For Xf, removal of $Ag^+$ from $m = 3.5$ in borate left a significant decrease in infectivity, yet the sedimentation and spectral changes were fully restored. However, when Xf was titrated to $m = 3.0$ in phosphate, no infectivity loss was observed. For Pf1, no loss of infectivity was noted when $Ag^+$ was removed after having been added to $m = 3.5$, but the samples showed increased light scattering and CD spectra with increased negative ellipticity for 250–300 nm.

*$Ag^+$ Binding to IKe and If1 Viruses.* The CD and difference absorbance spectra of the Ag–IKe and Ag–If1 complexes are shown in Figures 8 and 9, respectively. The CD and absorbance curves for both viruses are very similar to those described for the Ag–fd complexes. Addition of $Ag^+$ to IKe resulted in sedimentation increases of 7.5% and 11.2% at $m = 0.5$ and $m = 1.0$, respectively. The binding of $Ag^+$ to IKe showed slow kinetics effects. No loss of infectivity was observed for the IKe samples titrated with $Ag^+$.

*$Ag^+$ Binding to Pf3 Virus.* We previously reported that addition of $Ag^+$ to Pf3 causes large changes in light scattering but no changes in the CD spectra of the virus, as if the DNA in Pf3 were not accessible to $Ag^+$ (Casadevall & Day, 1982). Futher studies have shown, however, that some preparations do not exhibit the increases in light scattering but do give absorbance changes observed for $Ag^+$ binding to DNA. The decrease in absorbance for these preparations of Pf3 at 250 nm (Figure 10) is larger than that of any of the other viruses except Pf1 (Casadevall & Day, 1982). The absorbance changes for $m < 0.71$ are different from those for $1.19 < m < 2.4$ (Figure 10). CD changes accompanying the large absorbance effects were small (Figure 10) and unlike any other virus or DNA sample. Increases in sedimentation velocity of 5% and 11% occurred at $m = 0.25$ and 0.5, respectively. The absorbance and sedimentation changes for these samples were reversible.

*$Hg^{2+}$ Binding to Double- and Single-Stranded DNA.* Addition of $Hg^{2+}$ to double-stranded, superhelical PM2 DNA in 0.15 M borate, pH 8.6, buffer resulted in absorbance and CD spectra (data not shown) which are very similar to those reported for $Hg^{2+}$ complexes with DNA (Yamane & Davidson, 1961; Nandi et al., 1965; Walter & Luck, 1977). The absorbance changes involved increased absorbance centered at 290 nm and decreased absorbance at 250 nm. The difference absorbance spectra of the Hg–dsDNA for $0 < m <$

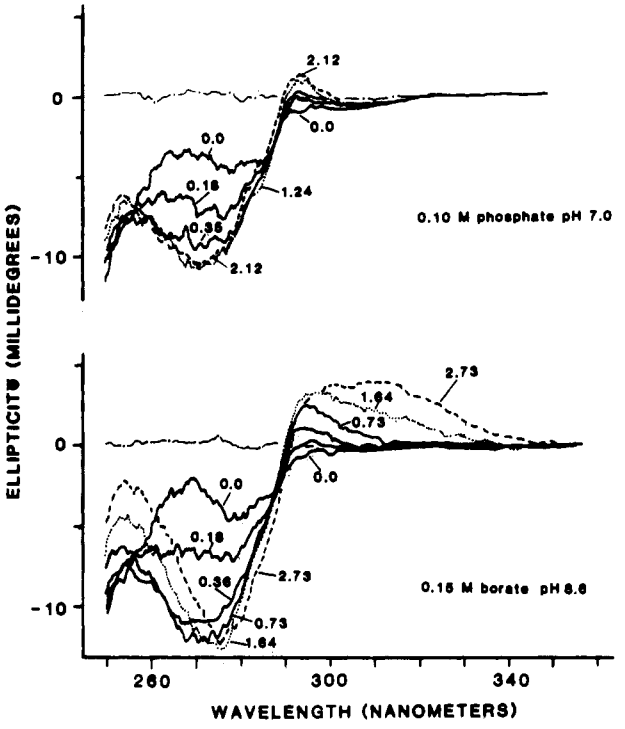


FIGURE 6: CD spectra of the Ag–Pf1 complexes in pH 8.6, 0.15 M borate and pH 7.0, 0.10 M phosphate buffers at various values of $m$. The virus concentration in each buffer was 0.35 mg/mL, which corresponds to 0.021 mg/mL DNA. The average total molar ellipticity change at 275 nm for four different Pf1 samples was −12 500 ± 1400 in borate. The total molar ellipticity change of the sample in phosphate was −9300. (See Figure 5 for a minor correction to a previously published CD spectrum of Pf1.)

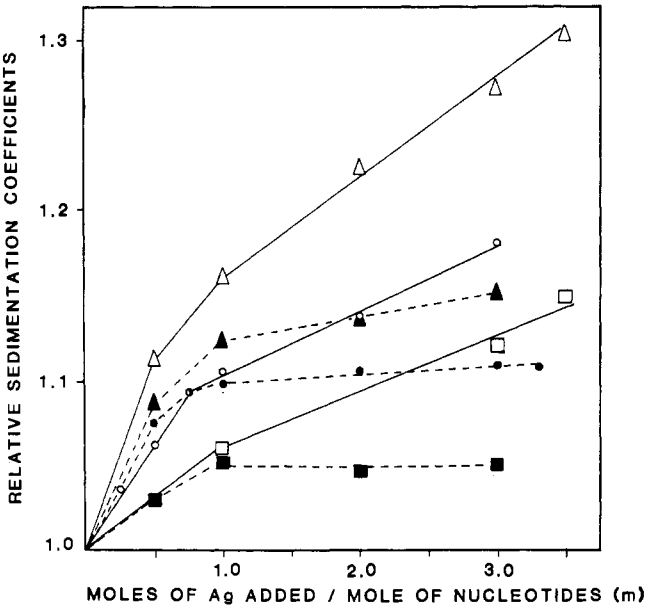


FIGURE 7: Plot of relative sedimentation coefficients vs. $m$. The triangles, circles, and squares are for to the Xf, fd, and Pf1 viruses, respectively. The filled symbols are for phosphate buffer, and the open symbols are for borate buffer. The Xf, fd, and Pf1 concentrations used in the sedimentation runs were 0.12, 0.13, and 0.20 mg/mL, respectively.

0.5 were isosbestic at 240.5 and 261 nm, whereas those for $m > 0.5$ had no well-defined isosbestic points. The total ellipticity change at 285 nm reached −56 500 deg cm$^2$ dmol$^{-1}$ for $m = 0.9$. Continued addition of $Hg^{2+}$ to $m > 0.9$ led to a decrease in the amplitude at 285 nm, such that at $m = 1.2$ the amplitude was −52 000 deg cm$^2$ dmol$^{-1}$. When $Hg^{2+}$ was

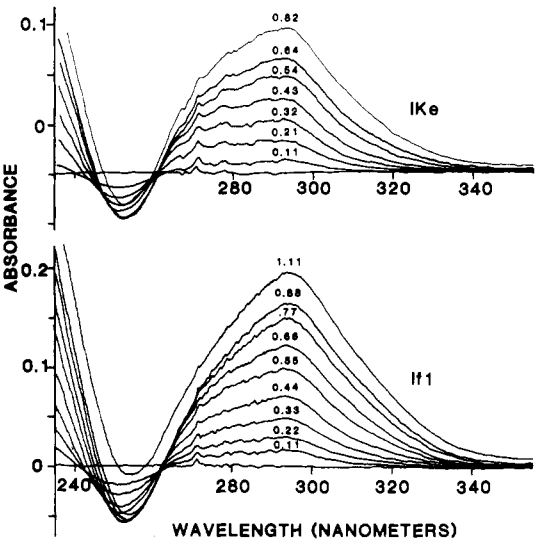


FIGURE 8: Difference absorbance spectra of Ag–IKe and Ag–If1 complexes in pH 8.6 borate buffer. The concentrations of the IKe and If1 viruses were 0.22 mg/mL (DNA concentrations 0.027 mg/mL). The optical path length was 1.0 cm.

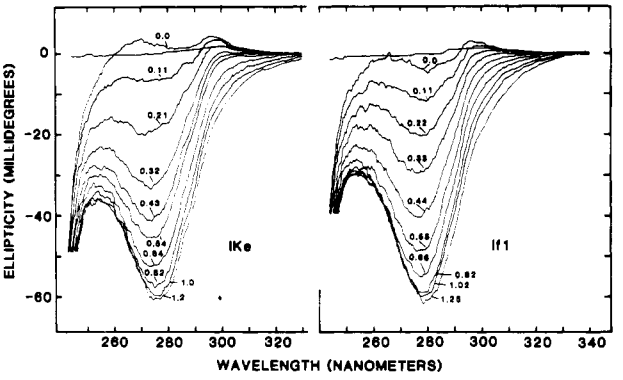


FIGURE 9: CD spectra of the IKe and If1 viruses and their complexes in 0.15 M borate, pH 8.6, buffer. The virus concentrations were 0.22 mg/mL, and the optical path length was 1.0 cm. For both viruses the maximum change in ellipticity at 277 nm was −70 000 deg cm$^2$ dmol$^{-1}$.

added to ssDNA, it induced absorbance and CD changes which were very similar to those observed for the Hg–dsDNA complexes, and these are shown in Figure 11. The difference spectra of the Hg–ssDNA complexes differ from those of the Hg–dsDNA complexes in that they show no clear isosbestic points. The large absorbance changes are paralleled by the formation of large negative bands in the CD spectra centered at 285 nm and 215 nm. The maximum negative amplitudes occur at 285 nm for values of $m \sim 0.5$, and then the amplitude slowly decreases with continued addition of $Hg^{2+}$.

*$Hg^{2+}$ Binding to fd, Xf, IKe, and If1.* The CD spectra of the Hg–fd and Hg–Xf complexes in a pH 8.6, 0.15 M borate buffer are shown in Figure 12. For $m < 0.8$, the addition of $Hg^{2+}$ causes a large decrease in ellipticity which is centered around 285 nm. The CD spectra in this range show considerable detail and appear to be the result of a negative band superimposed on the original fd virus spectrum. The CD changes have a well-defined end point near $m = 0.5$, after which no further changes in ellipticity occur until $m > 0.8$, when continued addition of $Hg^{2+}$ led to a decrease in amplitude. Changes for Xf involve a decrease in ellipticity in the 260–360-nm range, with a large negative band centered at around 290 nm. This band increases in amplitude up to $m = 0.66$, after which it reverses and begins to decrease in am-

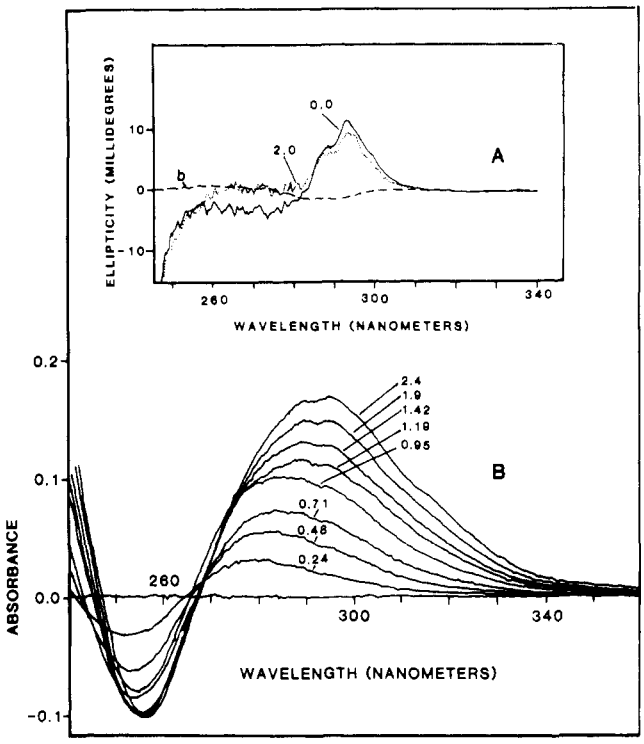


FIGURE 10: CD and difference absorbance spectra of Ag–Pf3 complexes in 0.15 M borate buffer, pH 8.6. (A) CD spectra of Ag–Pf3 complexes at $m = 0.0$ and $m = 2.0$. The Pf3 concentration was 0.38 mg/mL, which corresponds to a DNA concentration of 0.046 mg/mL. The optical path was 1 cm. Three spectra recorded for $0 < m < 2.0$ lay between the two spectra shown above. The molar ellipticity change at 270 nm induced by $Ag^+$ was +2400 deg cm$^2$ dmol$^{-1}$. The letter "b" denotes the buffer base line. (See legend to Figure 5 for a correction to a previously published spectrum of Pf3 virus.) (B) Difference absorbance spectra at various values of $m$. The concentration of virus was 0.211 mg/mL which corresponds to 0.025 mg/mL DNA. The optical path length was 1.0 cm.

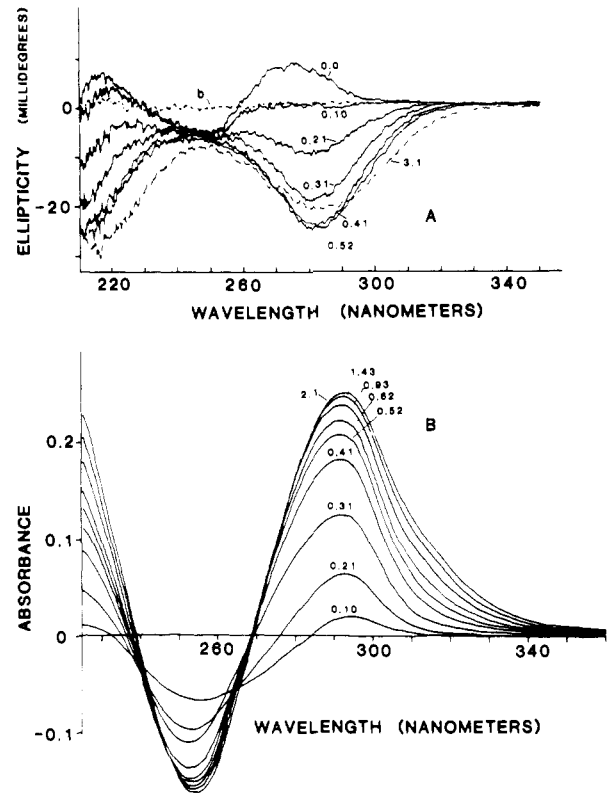


FIGURE 11: CD and difference absorbance spectra of Hg–ssDNA complexes at various values of $m$ in 0.15 M borate, pH 8.6, buffer. (A) CD spectra of Hg–ssDNA complexes. The initial ($m = 0.0$) and final ($m = 3.1$) DNA concentrations were 0.023 and 0.021 mg/mL, respectively. At $m = 0.52$, the total change in ellipticity at 283 nm was −41 200 deg cm$^2$ dmol$^{-1}$ and at $m = 3.1$ was −38 000 deg cm$^2$ dmol$^{-1}$. The optical path length was 1.0 cm. The letter b denotes the buffer base line. (B) Difference absorbance spectra of Hg–ssDNA complexes. The initial and final DNA concentrations were 0.23 and 0.0214 mg/mL, respectively. The optical path length was 1.0 cm.

plitude. For $m > 0.66$, the CD minimum of the Hg–Xf complexes undergoes a red shift such that for $m = 2.0$ it occurs at 305 nm. The changes in amplitude for fd, −38 600 deg cm$^2$ dmol$^{-1}$ at $m = 0.8$ are larger than those seen for the Xf complexes, −26 600 deg cm$^2$ dmol$^{-1}$. The difference absorbance spectra of the Hg–fd and Hg–Xf complexes corresponding to the CD spectra of Figure 12 are shown in Figure 13. The difference spectra for the Hg–fd complexes give no indication of the two different types of binding observed by CD. For $0 < m < 3.0$, there is an increase in absorbance at 290 nm and a decrease at 250 nm. The difference absorbance spectra for the Hg–Xf complexes in the $m < 0.66$ range are similar to those for Hg–fd complexes. For $m > 0.66$, some differences are seen; namely, the absorbance begins to increase at 250 nm such that for $m = 2.2$ the complexes no longer show an absorbance decrease at that wavelength, and the absorbance increase at 290 nm is split into two peaks which occur at 288 and 295 nm. Unlike $Ag^+$ binding, $Hg^{2+}$ binding to fd and Xf causes no increases in light scattering above $m = 0.5$. Addition of $Hg^{2+}$ to fd solutions in pH 5.0 or pH 5.5, 0.15 M acetate buffers caused CD and absorbance changes similar in shape and magnitude to those described above, but gellike aggregates were observed. In contrast, titrations of Xf with $Hg^{2+}$ did not produce aggregates.

$Hg^{2+}$ binding to fd and Xf viruses causes significant changes in sedimentation velocity. At $m = 0.5$, the sedimentation coefficients of the fd and Xf are increased by 10% and 20%, respectively, whereas at $m = 1.0$, the increases are 22% and 27%, respectively.

If1 and IKe were also found to react with $Hg^{2+}$ and yield complexes with absorbance and CD spectra very similar to those of the Hg–fd complexes (data not shown).

*$Hg^{2+}$ Binding to Pf1.* Addition of $Hg^{2+}$ to Pf1 solutions also results in changes to the CD spectra of the virus, but here the changes are smaller and very different from those observed for fd and Xf. The CD changes involve a decrease in ellipticity at 270 nm and a small increase in ellipticity at 305 nm. The band at 270 nm does not show the decrease in amplitude observed for the Hg–fd and Hg–Xf complexes for high values of $m$. The difference absorbance changes are also shown in Figure 13. The small CD changes (Figure 14) are paralleled by absorbance changes which are greater in magnitude than those for fd and Xf, as shown in Figure 13. At $m = 0.5$ and $m = 1.0$ the sedimentation velocity increased were 5% and 13.5%, respectively. As with the other viruses, addition of $Hg^{2+}$ did not cause increases in light scattering. When $Hg^{2+}$ was added to the Pf1 virus in slightly acidic acetate buffers, the viscosity of the solution increased drastically with successive increments of $Hg^{2+}$.

*$Hg^{2+}$ Binding to Pf3.* We have studied $Hg^{2+}$ binding to Pf3 using the same preparations in which the virions were found to be penetrable by $Ag^+$. Like Pf1, addition of $Hg^{2+}$ to Pf3 solutions results in large changes to the absorbance spectra of the virus but only small changes in the CD spectra. The difference absorbance and CD spectra of the Hg–Pf3 complexes are shown in Figure 15, respectively. The absorbance changes are very different from those of the other viruses and isolated DNAs, being positive at 270 nm. $Hg^{2+}$ binding causes

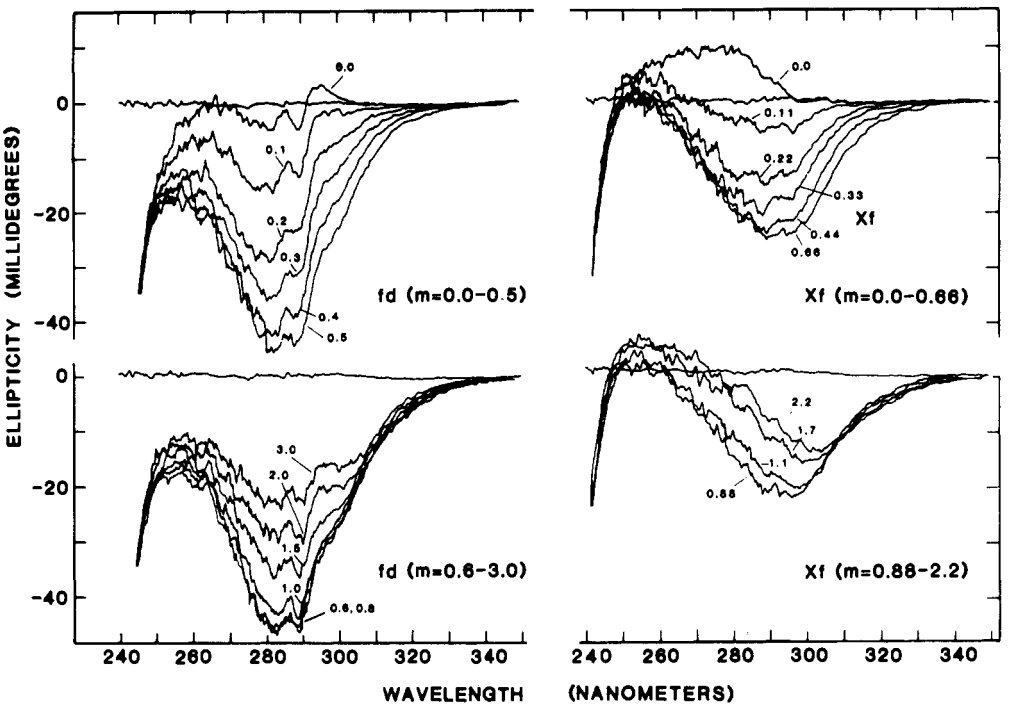


FIGURE 12: CD spectra of the Hg–fd and Hg–Xf complexes at various values of $m$ in 0.15 M borate, pH 8.6, buffer. The fd and Xf virus concentrations were 0.28 and 0.27 mg/mL, respectively, which corresponds to DNA concentrations of 0.034 and 0.035 mg/mL, respectively. At $m$ = 0.8 the total change in ellipticity for the Hg–fd complexes was −38 600 and −17 4000 deg cm$^2$ dmol$^{-1}$ at $m$ = 3.0. The largest change in amplitude observed for the Hg–Xf complexes occurred at $m$ = 0.66 where the total change in ellipticity at 290 nm was −25 400 deg cm$^2$ dmol$^{-1}$. The optical path length was 1 cm.

sedimentation changes. For $m$ = 0.5 and $m$ = 1.0 the sedimentation increases 9.8% and 26%, respectively.

*Reversibility.* Plaque assays revealed no loss of infectivity in fd, Xf, and Pf1 samples to which $Hg^{2+}$ had been added to $m$ = 1.0. The CD changes and the increase in sedimentation velocities were reversible when the $Hg^{2+}$ was removed. The large absorbance changes for all virus samples were also reversible although sometimes increased light scattering remained after the metal ion was removed and in some Pf1 samples slight changes near 266 nm persisted.

*Detergent Disruption of the $Hg^{2+}$ Complexes with fd, Xf, and Pf1.* Addition of the detergent sodium dodecyl sulfate (SDS) to fd, Xf, and Pf1 virus solutions already containing added $Hg^{2+}$ produced CD spectra expected for mixtures of Hg–DNA and free protein. Since the CD spectra of the Hg–fd complexes already look very similar to the Hg–DNA spectra, the change produced by the SDS addition was not large. Addition of SDS to Hg–Xf and Hg–Pf1 complexes resulted in larger CD changes as the spectra change presumably through changes in the DNA structure and in the way $Hg^{2+}$ is bound to the DNA. All the viruses are quite sensitive to SDS disruption, with concentrations of 0.02% SDS or less are required to produce the CD changes.

## Discussion

This study involved $Ag^+$ and $Hg^{2+}$ binding to six filamentous viruses and three types of DNA. Because of the amount of data and the details to be considered, the results of the $Ag^+$ and $Hg^{2+}$ experiments will be first discussed separately. Considerations of virus structure drawn from both sets of experiments will then be presented. A brief summary of all the observations and conclusions is given at the end.

### (*I*) *$Ag^+$ Binding to Isolated DNAs and to Viruses*

Ag–DNA data, from earlier studies and this study, provide information necessary for interpreting the Ag–virus data. Especially pertinent are the characteristics of the three types, or modes, of $Ag^+$ binding to dsDNA which occur at different ratios of bound $Ag^+$ per nucleotide, $r$. The predominant complexes are type I for $r < 0.2$, type II for $0.2 < r < 0.5$, and type III for $r > 0.5$ (Yamane & Davidson, 1962; Duane et al., 1966; Jensen & Davidson, 1966). Spectral characteristics of type I are an increase in absorbance at 285 nm and a decrease at 250 nm; for type II, absorbance increases throughout the ultraviolet region; for type III, absorbance decreases at 260 nm with an isosbestic point around 270 nm. The absorbance changes for types I and II are paralleled by two large negative CD bands centered near 220 and 270 nm (Minchenkova et al., 1969; Ding & Allen, 1980b). Heretofore, type III complexes have not been well-defined, partly because precipitates formed when the ratio of added $Ag^+$ per nucleotide, $m$, exceeded 0.5 in buffers used by previous investigators (Jensen & Davidson, 1966; Matsuoka & Norden, 1983). [In probing several viruses and DNAs under various buffer conditions in this study, we did not attempt to determine "$r$", the number of $Ag^+$ actually bound per nucleotide. However, the association constants for $Ag^+$ binding to dsDNA are high (Yamane & Davidson, 1961; Poletaev et al., 1969) and for the dsDNA concentration used, $m$ is a close approximation to $r$ up to $m \sim 0.8$ in borate buffers and up to $m \sim 0.5$ in phosphate buffers).

*CD and Absorbance Characteristics of Type III Ag–DNA Complexes.* The CD spectra of Ag–dsDNA complexes for $m < 0.5$ (binding types I and II) have large negative bands centered at 216 and 269 nm, and most of this change occurs for $0.2 < m < 0.5$, the range over which formation of the type II complexes predominates. By $m \sim 0.5$, type I and type II sites are saturated. One can assign to type III binding the absorbance and CD spectral shifts which occur on the binding of additional $Ag^+$ ions to saturated type I and type II Ag–dsDNA complexes. By using 0.15 M borate buffers at pH 7.5 and pH 8.6, we could avoid the formation of precipitates

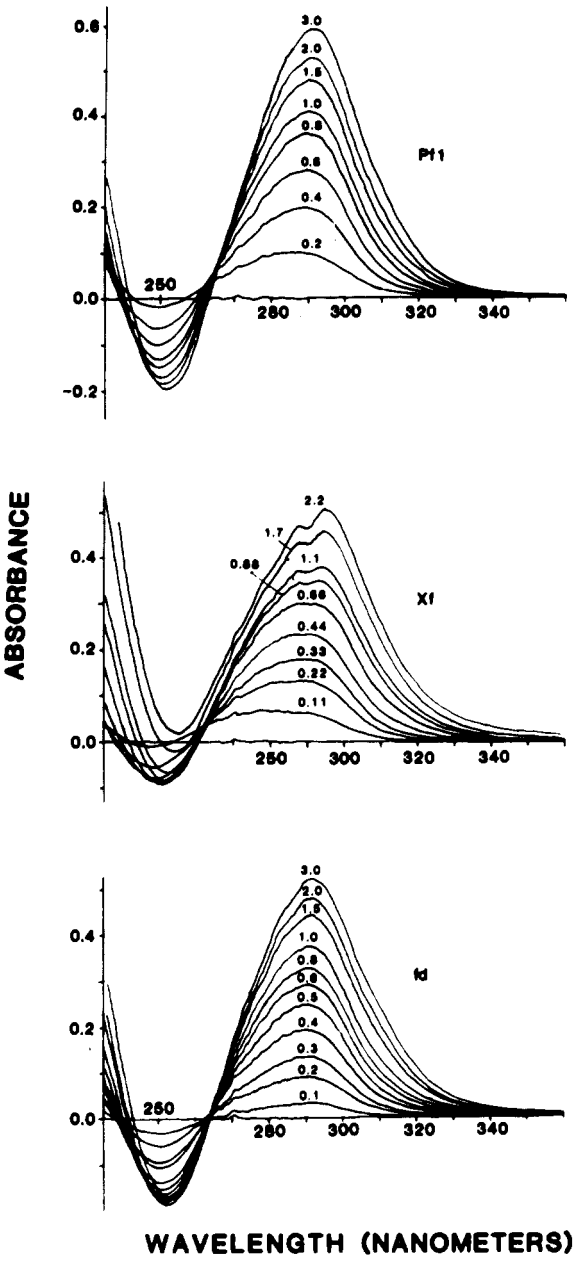


FIGURE 13: Difference absorbance spectra of Hg–Pf1, Hg–Xf, and Hg–fd complexes in 0.15 M borate, pH 8.6, at various values of $m$. The conditions for these titrations are the same as described in the legends to Figures 3 and 5, and these absorbance spectra correspond to these CD spectra. The optical path length was 1 cm.

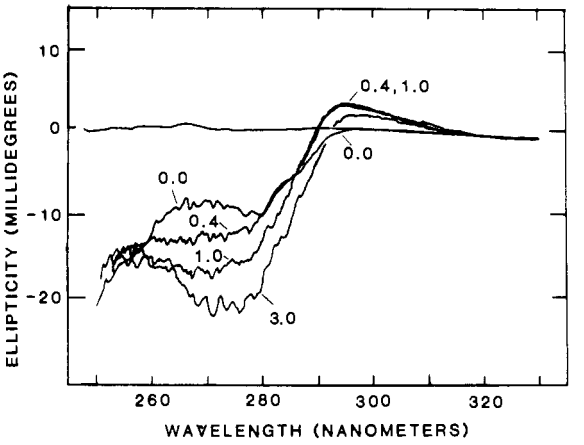


FIGURE 14: CD spectra of Hg–Pf1 complexes in 0.15 M borate, pH 8.6, at various values of $m$. The virus concentration was 0.55 mg/mL which corresponds to a DNA concentration of 0.033 mg/mL. The total change in ellipticity at 275 nm was −11 100 deg cm$^2$ dmol$^{-1}$ at $m$ = 3.0. The maximum change in ellipticity at 297 nm was approximately +3000 deg cm$^2$ dmol$^{-1}$, and it occurred for $m$ = 0.4–1.0. The optical path length was 1.0 cm.

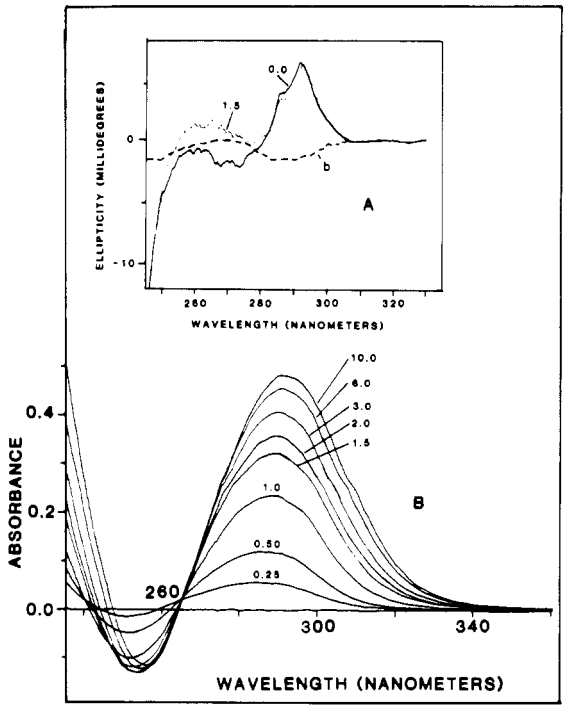


FIGURE 15: CD and difference absorbance spectra of Hg–Pf3 complexes in 0.15 M borate, pH 8.6, buffer. (A) The CD spectra corresponding to $m$ = 0.0 and $m$ = 1.5 are labeled. Spectra for 0 < $m$ < 2.0 occurred between those for $m$ = 0.0 and $m$ = 1.5. The virus concentration was 0.218 mg/mL corresponding to a DNA concentration of 0.0262 mg/mL. The optical path length was 1 cm. The letter b denotes the buffer base line. The $m$ = 1.5 spectra corresponds to that of the same value of $m$ in Figure 6. (B) Difference absorbance spectra of Hg–Pf3 complexes in 0.15 M borate, pH 8.6, buffer. The virus concentration was 0.218 mg/mL. The initial and final DNA concentrations were 0.0262 and 0.0257 mg/mL. The optical path length was 1 cm.

reported by others for $m > 0.5$. As $Ag^+$ is added beyond $m$ = 0.5 in borate buffer, the difference absorbance spectra become isosbestic at 269 nm (Figure 1) and show long wavelength tails. In the corresponding CD spectra (Figure 2), the two negative bands are shifted to 220 and 283 nm, with isosbestic points arising at 245 and 275 nm on the shift; there are also long wavelength tails. The presence of isosbestic points in the absorbance and CD spectra of the Ag–dsDNA complexes for 0.55 < $m$ < 1.1 clearly shows the existence of different binding sites and/or conformational states for $m >$ 0.5 as compared to $m < 0.5$. We call this type III binding and assign it a molar extinction coefficient increase of about 2500 $M^{-1}$ $cm^{-1}$ at 296 nm when $m$ is increased beyond 0.5 up to final saturation; over this whole range the wavelength of the maximum absorbance change is near 296 nm. Furthermore, beginning at $m$ = 0.5, the maximum CD change occurs at 293 nm, with $\Delta[\theta]$ per nucleotide of approximately −43 000 deg cm$^2$ dmol$^{-1}$. We also assign to type III binding the long wavelength phenomena. In contrast, once again, no changes at all are observed beyong $m$ = 0.5 in phosphate buffer.

We do not know what causes the long wavelength phenomena. Below $m$ = 0.5 the difference absorbance and the CD amplitudes at, say, 320 nm are zero or nearly zero, but beyond $m$ = 0.5 significant amplitudes at this wavelength occur. The long wavelength effects extend out to approxi-

mately 350 nm. The difference absorbance amplitudes do not follow the wavelength dependence in the range 310–350 nm expected for turbidity (Camerini-Otero & Day, 1978), and the corresponding CD effects were measured here with a CD spectrometer having a relatively low collection angle in the forward scattering direction, a direction expected to give low or zero differential scattering of right-handed vs. left-handed circular polarized light (Tinoco et al., 1981). Therefore, the long wavelength phenomena are distinguished from light-scattering effects. (This aspect, as well as similarities in CD spectra of Ag–DNA complexes to those of certain condensed forms of DNA, will be dealt with elsewhere.)

*Subtle Differences between Ag–ssDNA and Ag–dsDNA Complexes.* We have previously argued that the overall similarities in the CD spectra of Ag–dsDNA and Ag–ssDNA complexes are due to the fact that $Ag^+$ can form the same types of complexes with ssDNA and dsDNA (Casadevall & Day, 1982). Nevertheless there are distinguishable differences between the Ag–dsDNA and Ag–ssDNA complexes: (1) the CD spectra of the Ag–ssDNA complexes exhibit long wavelength tails for $m > 0.3$ whereas the CD of the Ag–dsDNA complexes exhibit them later in the titration, for $m > 0.5$ (this holds for borate buffer only, since phosphate buffer suppresses long wavelength tails for dsDNA and ssDNA); (2) prominent isobestic points are present in the CD and absorbance spectra for Ag–dsDNA, but for Ag–ssDNA the corresponding points appear washed out; (3) molar ellipticities at the various minima are smaller for Ag–ssDNA complexes; (4) the ssDNA complexes exhibit a large decrease in absorbance at 250 nm, but dsDNA complexes do not. Whereas types I and III have a decrease in absorbance at 250 nm, type II binding has an increase at 250 nm. The Ag–dsDNA complexes at pH 8.6 do not show a decrease in absorbance at 250 nm for $m > 0.2$, probably because the type II absorbance changes counteract those of type I. The decrease in absorbance at 250 nm for ssDNA at pH 8.6 is probably the result of fewer type II sites in Ag–ssDNA than in Ag–dsDNA. We assign the long wavelength tails in the CD spectra of some Ag–ssDNA complexes to the simultaneous occurrence of type II and type III binding.

*Nature of $Ag^+$ Binding Sites.* Various proposals for type I sites are N3 and N7 $\sigma$ electrons of purines (Yamane & Davidson, 1962), the $\pi$ systems of the bases (Jensen & Davidson, 1966), and chelation of the $Ag^+$ between N7 and the keto oxygen of guanines (Jensen & Davidson, 1966; Ding & Allen, 1980a; Dattagupta & Crothers, 1981). There is more agreement on type II sites. Formation of the type II complexes, but not the others, is accompanied by proton release and is believed to involve the formation of a Ag bridge between bases in opposite strands (Yamane & Davidson, 1962; Albiser & Premilat, 1976; Shin & Eichhorn, 1980). A recent review on this subject is that of Marzilli et al. (1980). We have no proposal for the nature of type III sites other than they are sites which are available after type I and type II sites are saturated or nearly so. The fact that the characteristic features of type III binding are observed for superhelical DNAs, in which the right-handed helical sense of the fundamental helix cannot change due to covalent closures of both strands and the fixed linking number, means that they are for right-handed, base–base stacked helical Ag–DNA complexes. The finding that CD spectra of Ag–ssDNA and Ag–dsDNA are so similar indicates that the complexes that Ag forms with ssDNA are also right-handed helices.

The exact structure of the various Ag–DNA complexes will remain uncertain until more X-ray diffraction studies of $Ag^+$ complexes with nucleotides, oligonucleotides, and DNA are undertaken. The finding that type III occurs in alkaline borate buffers but not in neutral phosphate buffers may be useful since it allows the preparation of Ag complexes which have or lack the type III complex. The buffer-dependent effect is probably the result of a complex equilibrium where $Ag_3PO_4$ is formed and precipitates after the type I and type II binding sites are saturated. Thus, buffer type as well as pH can be manipulated to change the relative amounts of type I, type II, and type III binding.

*$Ag^+$ Probing of DNA Structures in the Six Viruses.* We observed earlier for both fd and Xf that the increase in negative ellipticity upon $Ag^+$ binding at 275 nm was about 80% that for Ag–dsDNA, and this major change in amplitude was considered to be from type II binding. $Ag^+$ bridges proposed form between bases in opposite strands, although the bases are not all complementary in the Watson–Crick sense. The $Ag^+$ complexes of both viruses show long wavelength CD tails. With the present results, we interpret the occurrence of the long wavelength phenomena in Ag–fd and Ag–Xf spectra to be due to binding like that assigned to type III for dsDNA. From this more detailed analysis we strengthen our earlier conclusion that the helical sense of the DNAs in fd and Xf is right handed.

The Ag–IKe and Ag–If1 complexes have CD spectra very similar to those of Ag–fd, a result which is not surprising in view of the fact that all these viruses produce the same type of X-ray diffraction pattern and are class I filamentous viruses (Marvin et al., 1974). The $Ag^+$ binding results indicate that the DNAs in IKe and If1 are packed as in fd, in right-handed helices having pitches near 27 Å with the bases directed toward the structure axes. The kinetic effects observed for $Ag^+$ binding to the DNA inside the IKe virion, however, indicate some differences in structure between fd and IKe.

For Pf1, the combined CD and absorbance changes are very different from those observed in the other systems. Most striking is that ellipticity changes are, by comparison to dsDNA, very small yet absorbance changes are very large. An electronic transition near 293 nm is enhanced, but it is non-chiral. CD changes characteristic of type II and type III binding are entirely absent. The unusual positive long wavelength CD band could be suppressed in phosphate buffer. On the basis of the $Ag^+$ probing alone, we conclude that the Pf1 DNA structure is unique.

For Pf3, we found earlier that of $Ag^+$ caused large increases in light scattering but no true absorbance and CD changes. Since then we have found some Pf3 preparations for which the protein coat is penetrable by $Ag^+$. These virus samples have the same initial absorbance and CD spectra and the same appearance by EM and sediment at the same rate as samples that are nonpenetrable by $Ag^+$. Their plating efficiencies, however, are very low, only 1 or 2% as compared to the usual 10–65%. Approximately half the major coat protein subunits in the penetrable virions have a few amino acids missing from their N-terminal ends (B. Frangione, personal communication). The fortunate availability of these poor Pf3 preparations has allowed us to probe the DNA packing with $Ag^+$. The data show that $Ag^+$ binds to the DNA, inducing very large changes in absorbance but only very small changes in CD. The small CD changes are quite different from the small CD changes for Pf1. From these observations, we conclude that the Pf3 DNA structure is also unique.

*(II) $Hg^{2+}$ Binding to Isolated DNA and to the Viruses*

*How $Hg^{2+}$ Binds to DNA.* Before discussing $Hg^{2+}$ binding to the viruses and its implications for structure, we outline what is known about $Hg^{2+}$ binding to DNA. When $Hg^{2+}$ binds to double-stranded DNA, it does so in at least two distinguishable modes, one when the mole ratio of $Hg^{2+}$ bound per nucleotide, $r$, is less than 0.5 and the other when $r > 0.5$ (Yamane & Davidson, 1961; Nandi et al., 1965). The formation of the first complex, but not the second, is accompanied by the release of two protons for each $Hg^{2+}$ bound (Yamane & Davidson, 1961). The CD changes involve the formation of two large negative bands centered at 215 and 285 nm, respectively, each of which reach their maximum amplitude at $r = 0.7$–0.8 and decreases in amplitude with continued binding of $Hg^{2+}$ (Simpson & Sober, 1970; Walter & Luck, 1977; Ding & Allen, 1980a,b). The mechanism of binding probably involves $Hg^{2+}$ ions binding between bases to form bridges between opposite strands (Yamane & Davidson, 1961; Nandi et al., 1965; Luck & Zimmer, 1971). The binding of $Hg^{2+}$ to poly(dA-dT) has been proposed to cause chain slippage with the formation of interstrand thymidine–Hg–thymidine complexes (Katz, 1963). The existence of thymidine–Hg–thymidine complexes where the Hg is bound to the N3 atom has been shown by X-ray crystallography of a 2:1 complex of 1-methylthymidine–Hg (Kosturko et al., 1974). Kinetics of $Hg^{2+}$ binding to polynucleotides have also been interpreted in terms of bridge formation (Williams & Crothers, 1975). Recently, an NMR study of Hg(II) binding to poly(dA-dT) has shown that N3 is indeed the binding site and that interstrand cross-linking occurs (Young et al., 1982).

*$Hg^{2+}$ Binding to Six Filamentous Viruses.* The absorbance changes induced by $Hg^{2+}$ binding to fd, If1, IKe, Xf, Pf1, and Pf3 viruses are very similar to those reported for $Hg^{2+}$ binding to isolated DNAs, whether double stranded or single stranded. Single-stranded fd DNA isolated from the virus binds $Hg^{2+}$ and forms complexes which have very similar absorbance and CD spectra as those resulting from $Hg^{2+}$ binding to dsDNA. This indicates that $Hg^{2+}$ forms the same types of complexes with ssDNA and dsDNA. This result is not surprising since fd ssDNA in solution has considerable secondary structure including a 20 base paired hairpin, and thus provides $Hg^{2+}$ with similar binding sites as dsDNA. Furthermore the CD spectra of the mercury complexes with four of the viruses (fd, If1, IKe, and Xf) are very similar to those of Hg–DNA complexes. The aggregation and gel phenomena seen in low pH buffers for fd and Pf1 viruses may indicate some interactions between $Hg^{2+}$ and the protein components. However, only slight, if any, changes in CD were observed for fd, IKe, and Pf1, the only viruses tested, over the range dominated by protein contributions, 200–240 nm (unpublished observations). There is no sulfhydryl group in the major coat protein of any of these phages, and although other possible mercury binding sites such as carboxylate and amino groups exist, the association constants for the binding of $Hg^{2+}$ to such groups are much smaller than those for binding to the DNA bases. Thus, in the absence of protein sites which can compete effectively with the DNA bases and in view of the spectral data, we conclude that $Hg^{2+}$ ions are binding predominantly to the bases inside the virions.

The fact that the CD spectra of the Hg–fd, Hg–If1, Hg–IKe, and Hg–Xf complexes are similar to those of the Hg–DNA indicates that $Hg^{2+}$ is forming the same types of complexes with the DNA inside those viruses as with DNAs in solution. $Hg^{2+}$ can form interstrand bridges between opposing bases when it binds to dsDNA. The reversible formation of Hg–DNA complexes inside the fd, If1, IKe, and Xf viruses without disruption indicates that the bases in these virions are detected toward the structure axis. However, in contrast to the virtually identical CD and absorbance spectra for Ag–fd and Ag–Xf, the CD and absorbance spectra of their Hg complexes shows small, but reproducible, differences. These differences are not understood, but their origin may lie in the different base compositions of fd ssDNA [24.6% A, 34.5% T, 20.7% G, and 20.2% C; calculated from the data of Beck et al. (1978)] and Xf ssDNA (21% A, 19% T, 33% G, and 27% C; Kuo et al., 1971). CD spectra of various Hg–polynucleotide complexes show different shapes (Walter & Luck, 1978), and $Hg^{2+}$ forms spectrally different complexes with the DNA nucleosides (Eichhorn & Clark, 1963; Simpson, 1964). For example, $Hg^{2+}$ forms bridges preferentially between thymidines (Young et al., 1982), and the probability that two thymidines are in a position conducive to bridge formation is greater in fd than in Xf.

The different CD spectra of the Hg–Pf1 complexes indicate that a very different DNA structure exists in this virion. Similarly, the CD spectra of the Hg–Pf3 complexes are so different from those of the other viruses that Pf3 must also have a very different DNA structure.

### (*III*) *Considerations Based on both $Ag^+$ and $Hg^{2+}$ Results*

*I-Form DNA in Pf1 and Pf3.* One can assign relatively high molar nucleotide absorbances of 8000 and 8200 for the DNAs in Pf1 and Pf3, as compared to values near 6500 for fd and Xf, and for dsDNA (Day & Wiseman, 1978; Casadevall & Day, 1982). These findings, as well as Raman data (Thomas et al., 1983) and some fluorescence data (Day et al., 1979), are consistent with the absence of base–base stacking in Pf1 and Pf3, but its presence in fd and Xf. The spectral data, an axial nucleotide translation of greater than 5 Å in Pf1, the nature of the amino acid sequences of the major coat proteins of both Pf1 and Pf3, and considerations of DNA and protein symmetry in the virions have all led to the proposal of inverted DNA structures (I-form DNA) in Pf1 and Pf3 having bases out and phosphates in (Day et al., 1979, Marzec & Day, 1983; Putterman, 1983). The $Ag^+$ probing results presented herein are consistent with this proposal. The results show that the DNAs in Pf1 and Pf3 bind $Ag^+$ and $Hg^{2+}$ very differently from ssDNA and dsDNA in solution. The absence of large negative changes in the CD spectra as well as the features of the difference absorbance spectra of the Ag–Pf1 and Ag–Pf3 complexes indicate that the $Ag^+$ and $Hg^{2+}$ are not forming metal ion bridges between the two antiparallel DNA strands in these viruses.

*Influence of the Protein Sheath on $Hg^{2+}$ and $Ag^+$ Binding and DNA–Protein Linkage.* The viral protein sheath influences $Ag^+$ and $Hg^{2+}$ binding to the DNAs inside the viruses by determining the DNA structure and thus the types of complexes that can form. The protein coat is also responsible for the slow kinetic effects observed in $Hg^{2+}$ binding. In the case of some Pf3 preparations, the protein sheath completely prevents metal ion binding to the DNA. For fd, If1, IKe, and Xf, the CD changes caused by $Ag^+$ binding are so similar to those observed for $Ag^+$ binding to isolated DNAs in solution that it appears as though the protein sheath does not hinder binding in any way. For fd at least, we do know that the protein sheath rigidly holds the DNA in place (DiVerdi & Opella, 1981; Fritzche et al., 1981) and, if the same $Ag^+$ complexes form inside the virus as in isolated DNA, it is because the protein constrains the DNA in a conformation that allows it to do so. Although the protein sheath is ultimately

responsible for the type, the rate, and the extent of binding, we observed no detectable change in protein secondary structure when $Ag^+$ bound to fd, Pf1, and Pf3 and only a small increase in $\alpha$-helicity of Xf (Casadevall & Day, 1982). The large, reversible increases in sedimentation velocity upon $Ag^+$ and $Hg^{2+}$ binding bear on the subject of the linkage between the DNA and protein structures in the virions. The $Ag^+$ and $Hg^{2+}$ bind to the DNAs inside the virions yet cause the sedimentation rates for the whole virions to increase. The sedimentation changes are largest for Xf virus and smallest for Pf1, and they indicate that $Ag^+$ and $Hg^{2+}$ are not causing aggregation. In general, sedimentation rate increases could be due to increased mass, shortening of the virions, decreased partial specific volume, or increased flexibility. It is clear that increased mass due to $Ag^+$ and $Hg^{2+}$ cannot account for the large sedimentation increases observed. Since DNA comprises a small percentage of the mass of these viruses (6–13%), and given the magnitude of the decrease in partial specific volume of the DNA upon $Hg^{2+}$ binding (Matsuda & Takeuchi, 1967), the most the sedimentation rate could increase via this route is 2–3%. Although we cannot rule out some metal ion binding to the protein which may affect protein packing, the large sedimentation increases strongly suggest structural linkages between the DNA and protein components in these virions. The relative sedimentation increases caused by $Hg^{2+}$ binding are larger than those caused by $Ag^+$ binding. A similar result was observed when $Ag^+$ and $Hg^{2+}$ were used to probe the structure of nucleosomes (Ding & Allen, 1980b).

*On the Use of Ag– and Hg–Virus Complexes in Other Studies.* One problem encountered in the structure studies on the filamentous viruses is that the DNA percentage per virion is low, so that DNA contributions to X-ray diffraction patterns and electron micrographs are weak and difficult to assign. The availability of virions having metal ions bound to bases are expected to be useful in overcoming this limitation. The $Ag^+$ and $Hg^{2+}$ ions each has their merits. Whereas $Ag^+$ probing showed the DNA structures inside fd and Xf to be nearly identical, $Hg^{2+}$ probing has demonstrated differences, albeit small, between these two viruses. The Hg atoms in Hg–virus complexes are likely to produce stronger reflections in X-ray diffraction studies than Ag by virtue of their larger size. Also, for $r < 0.5$, $Hg^{2+}$ forms one type of complex with DNA whereas $Ag^+$ forms two, a fact that may make the analysis of X-ray diffraction data from Hg–virus complexes simpler than for Ag derivatives. As a rule, $Hg^{2+}$ titrations were cleaner and showed no significant increases in light scattering until high values of $m$, whereas $Ag^+$ binding often induced increased light scattering for $m > 0.5$. Hg–virus complexes may be useful in Raman spectroscopy, whereas Ag–virus complexes have proved unsuitable because of the photoreactivity of the Ag derivatives (G. J. Thomas, Jr., personal communication). Nevertheless, $Ag^+$ caused smaller structural changes as monitored by sedimentation velocity. In any case, the present results help delineate the conditions for the preparation of Ag–virus and Hg–virus complexes for study by other techniques and thus provide means for testing the proposals for the various DNA structures.

*Summary and Conclusions.* The results of this study, together with those of our earlier study (Casadevall & Day, 1982), show that (1) the DNA structures inside the fd, If1, IKe, and Xf viruses are similar to each other but very different from those inside Pf1 and Pf3, (2) the DNAs inside the fd, If1, IKe, and Xf viruses form the same types of complexes with $Ag^+$ and $Hg^{2+}$ as double-stranded DNA in solution, indicating that the bases are so arranged that Ag and Hg bridges can form between bases in the opposite strands, (3) the DNA helices in the fd, If1, IKe, and Xf viruses are right-handed, (4) the CD and absorbance changes observed for the $Ag^+$ and $Hg^{2+}$ complexes with the Pf1 and Pf3 viruses are consistent with inside out DNA structures (I-DNA) proposed for these virions, and (5) sedimentation velocity changes induced by $Ag^+$ and $Hg^{2+}$ strongly suggest that the DNA and protein components are linked in these virions.

Acknowledgments

We are grateful to Paula D. Boyle, Louise Dennis, Margarete Klein, Debra G. Putterman, and Roy Smith for their assistance with various aspects of this study.

**Registry No.** Ag, 7440-22-4; Hg, 7439-97-6.

References

Albiser, G., & Premilat, S. (1976) *C. R. Hebd. Seances Acad. Sci., Ser. D 282*, 1557–1560.

Beck, E., Sommer, R., Auerswald, E. A., Kurz, Ch., Zink, B., Osterburg, G., Schaller, H., Sugimoto, K., Sugisaki, H., Okamoto, T., & Takanami, M. (1978) *Nucleic Acids Res. 5*, 4495–4504.

Berkowitz, S. A., & Day, L. A. (1980) *Biochemistry 19*, 2696–2702.

Camerini-Otero, R. D., & Day, L. A. (1978) *Biopolymers 17*, 2241–2249.

Casadevall, A., & Day, L. A. (1982) *Nucleic Acids Res. 10*, 2467–2481.

Cassim, J. Y., & Yang, J. T. (1969) *Biochemistry 8*, 1947–1951.

Cross, T. A., Tsang, P., & Opella, S. J. (1983) *Biochemistry 22*, 721–726.

Dattagupta, N., & Crothers, D. M. (1981) *Nucleic Acids Res. 9*, 2971–2985.

Daune, M., Dekker, A., & Schachman, H. K. (1966) *Biopolymers 4*, 51–76.

Day, L. A., & Wiseman, R. L. (1978) in *The Single-Stranded DNA Phages* (Denhardt, D., Dressler, D., & Ray, D., Eds.) pp 605–625, Cold Spring Harbor Press, Cold Spring Harbor, NY.

Day, L. A., Wiseman, R. L., & Marzec, C. J. (1979) *Nucleic Acids Res. 7*, 1393–1403.

Ding, D., & Allen, F. S. (1980a) *Biochim. Biophys. Acta 610*, 64–71.

Ding, D., & Allen, F. S. (1980b) *Biochim. Biophys. Acta 610*, 72–80.

DiVerdi, J. A., & Opella, S. J. (1981) *Biochemistry 20*, 280–284.

Dorne, B., & Hirth, L. (1970) *Biochemistry 9*, 119–125.

Eichhorn, G., & Clark, P. (1963) *J. Am. Chem. Soc. 85*, 4020.

Fritzche, H., Cross, T. A., Opella, S. J., & Kallenbach, N. R. (1981) *Biophys. Chem. 14*, 283–291.

Katz, S. (1963) *Biochim. Biophys. Acta 68* 240–253.

Kosturko, L. D., Folzer, C., & Steward, R. F. (1974) *Biochemistry 13*, 3949–3252.

Kuo, T. T., Huang, R. Y., & Chow, T. Y. (1971) *Virology 39*, 548.

Jensen, R. H., & Davidson, N. (1966) *Biopolymers 4*, 17–34.

Luck, G., & Zimmer, C. (1970) *Eur. J. Biochem. 18*, 140–145.

Marvin, D. A., Wiseman, R. L., & Wachtel, E. J. (1974) *J. Mol. Biol. 82*, 121–138.

Marzec, C. J., & Day, L. A. (1983) *Biophys. J. 42*, 171–180.

Marzilli, L. G., Kistenmacher, T. J., & Eichhorn, G. L. (1980) in *Nucleic Acid-Metal Ion Interactions* (Spiro, T. G., Ed.) pp 179–205, Wiley, New York.

Matsuda, M., & Takeuchi, E. (1967) *J. Biochem. (Tokyo) 61*, 523-526.
Matsuoka, Y., & Norden, B. (1983) *Biopolymers 22*, 601-604.
Minchenkova, L. E., Belykh, R. A., Dobrov, E. N., & Ivanov, V. I. (1969) *Mol. Biol. (Moscow) 3*, 348-353.
Nandi, U. S., Wang, J. C., & Davidson, N. (1965) *Biochemistry 4*, 1687-1696.
Poletaev, A. I., Ivanov, V. I., Minchenkova, L. E., & Shchelkina, A. K. (1969) *Mol. Biol. (Moscow) 3*, 283-244.
Putterman, D. G. (1983) Ph.D. Dissertation, New York University.
Shin, Y. A., & Eichhorn, G. L. (1980) *Biopolymers 19*, 539-556.
Simpson, R. B. (1964) *J. Am. Chem. Soc. 86*, 2059.
Simpson, R. T., & Sober, H. A. (1970) *Biochemistry 9*, 3103-3109.
Thomas, G. J., Jr., Prescott, B., & Day, L. A. (1983) *J. Mol. Biol. 165*, 321-356.
Tinoco, I., Bustamante, C., & Maestre, M. F. (1981) *Annu. Rev. Biophys. Bioeng. 9*, 107-141.
Walter, A., & Luck, G. (1977) *Nucleic Acids Res. 4*, 539-550.
Walter, A., & Luck, G. (1978) *Stud. Biophys. 68*, 1-10.
Williams, N. M., & Crothers, D. M. (1975) *Biochemistry 14*, 1944-1950.
Yamamoto, K. R., Alberts, B. M., Benzinger, R., Lawhorne, L., & Treiber, G. (1970) *Virology 40*, 734-744.
Yamane, T., & Davidson, N. (1961) *J. Am. Chem. Soc. 83*, 2599-2607.
Yamane, T., & Davidson, N. (1962) *Biochim. Biophys. Acta 55*, 609-621.
Young, P. R., Nandi, U. S., & Kallenbach, N. R. (1982) *Biochemistry 21*, 62-66.

# High-Resolution Proton Nuclear Magnetic Resonance Analysis of Solution Structures and Conformational Properties of Mugineic Acid and Its Metal Complexes†

Takashi Iwashita, Yoshiki Mino, Hideo Naoki, Yukio Sugiura, and Kyosuke Nomoto*

ABSTRACT: Proton nuclear magnetic resonance ($^1$H NMR) spectral studies at 360 MHz have been conducted on mugineic acid and its Zn(II) and Co(III) complexes. Resonance assignments are presented for all the CH protons of mugineic acid on the basis of homonuclear spin decoupling and the *J*-resolved two-dimensional spectroscopic experiments. The conformational analysis using chemical shifts and vicinal coupling constants showed that (1) mugineic acid coordinates to Zn(II) and Co(III) ions in hexadentate fashion by the six functional groups and (2) the C1′–C2′, C1″–C2″, and C2″–C3″ bonds change from mixtures of rotamer populations in free mugineic acid to predominantely gauche–gauche populations in the metal complexes. The structural conformation of the mugineic acid–Co(III) complex in aqueous solution corresponds well to that of its crystal structure determined by X-ray diffraction technique.

Mugineic acid, (2*S*,2′*S*,3′*S*,3″*S*)-*N*-[3-carboxy-3-[(3-carboxy-3-hydroxypropyl)amino]-2-hydroxypropyl]azetidine-2-carboxylic acid, is a unique phytosiderophore that is excreted from the roots of barley (Takagi, 1976; Takemoto et al., 1978). Recent experiments demonstrated that (1) the $^{59}$Fe uptake in the rice root is remarkably stimulated by mugineic acid and (2) the addition of mugineic acid to the medium of water-cultured rice at pH 7.0 increases the chlorophyll content (Mino et al., 1983). Other graminaceous plants such as wheat and oats have also produced novel amino acids similar to mugineic acid from their roots in order to effectively absorb iron under the condition of iron deficiency (Nomoto et al., 1979; Fushiya et al., 1980). The coordination chemistry of this novel amino acid is essential to elucidate the mechanism of iron uptake and transport in graminaceous plants and/or the iron chlorosis induced by transition metals such as Cu(II) and Zn(II) ions (Hunter & Vergano, 1953). Although we previously clarified the X-ray crystal structures for the Cu(II) and Co(III) complexes of mugineic acid (Mino et al., 1981, 1983), the solution chemistry of mugineic acid and its metal complexes is uncertain. Proton nuclear magnetic resonance has proven to be of limited value for the study of mugineic acid–Fe(III) and –Cu(II) complexes because of their paramagnetic effects. However, the conformational changes of mugineic acid resulting from metal coordination can be studied by using Zn(II) and Co(III), since mugineic acid forms a tightly bound complex with these diamagnetic ions. Using the chemical shifts and coupling constants highly resolved by 360-MHz proton nuclear magnetic resonance ($^1$H NMR) spectra, in this paper, we have demonstrated the tertiary structure of mugineic acid and the conformational changes associated with metal binding in aqueous solution. The solution structure of the mugineic acid–Co(III) complex has also been compared with the structures determined by X-ray crystallographic analysis. The present information is prerequisite to understanding the conformation of biologically important mugineic acid–Fe(III) complex in aqueous medium and the mechanism of heavy metal induced iron chlorosis.

## Experimental Procedures

*Materials.* Mugineic acid was isolated and purified according to our previously reported procedures (Takemoto et al., 1978) and then was checked by field-desorption (FD) mass and NMR ($^1$H and $^{13}$C) spectra. All other reagents were the highest quality available.

*NMR Measurements.* $^1$H NMR spectra were obtained at 360 MHz on a Nicolet NT-360 NMR spectrometer equipped with a computer-controlled homonuclear decoupling accessory.

† From the Suntry Institute for Bioorganic Research, Shimamoto-cho Mishima-gun, Osaka 618, Japan (T.I., H.N., and K.N.), the Osaka College of Pharmacy, Matsubara-City, Osaka 580, Japan (Y.M.), and the Faculty of Pharmaceutical Science, Kyoto University, Kyoto 606, Japan (Y.S.). *Received May 10, 1983.*

0006-2960/83/0422-4842$01.50/0 